Oscillations of intersubband electron relaxation in a GaAs/Al$_x$Ga$_{1-x}$As wide single quantum well near the single- to double-layer transition

L. V. Kulik, L. V. Butov, A. A. Shashkin, and V. T. Dolgopolov

Institute of Solid State Physics, Russian Academy of Sciences, 142432 Chernogolovka, Russia

(Received 20 November 1997; revised manuscript received 2 February 1998)

We present the photoluminescence (PL) and transport study of an electron system confined in a high-quality wide single quantum well at $T \geqslant 60$ mK and $B \leqslant 14$ T. Near the single- to double-layer transition, if only one electron layer/subband is occupied in equilibrium, strong magneto-oscillations of the second-subband PL intensity with maxima around odd electron filling factors are observed at low temperatures $\lesssim 600$ mK. The shape of the oscillation maxima depends on intersubband energy spacing. The observed oscillations are shown to originate from the electron intersubband relaxation determined by the relative spin orientation of the initial and final electron states. [S0163-1829(98)51220-9]

Recently magnetotransport measurements of coupled bilayer electron systems in both wide single quantum wells (WSQW's) (Ref. 1) and double quantum wells (DQW's) (Ref. 2) have revealed a variety of intriguing phenomena originating from the new internal degree of freedom. The fractional quantum Hall states with even denominators as well as the phase transition at filling factor $\nu = 1$ caused by the interlayer Coulomb correlations have been observed in the symmetric, or balanced, double-layer regime where the electron distribution is two symmetric maxima corresponding to two electron layers.[1,2] Varying the WSQW potential profile in the z direction toward the asymmetric regime with the help of gate biases allows depopulation of one of the electron layers as shown in the inset to Fig. 1(b). In fact, for the strongly asymmetric WSQW both single- and double-layer regimes can be realized: (i) if electrons occupy only the lowest subband, the electron distribution is one maximum and the system is in the single-layer regime; (ii) if a second subband starts to collect electrons, the electron distribution is two asymmetric maxima and the system is in the unbalanced double-layer regime, see, e.g., Ref. 3. In the single-layer regime the WSQW is similar to either a single quantum well or a heterojunction with modulated doping. Both of the structures were used in intensive studies of the photoluminescence (PL) of a two-dimensional (2D) electron gas during the last decade (for a recent review see Ref. 4). The PL energy and intensity were found to oscillate at quantizing magnetic fields; these oscillations were regarded to be an optical analog of the Shubnikov–de Haas effect.[5–10] So far, the study of magneto-optical oscillations was largely focused on the case of even filling factors. This was creative for understanding such phenomena as the band-gap renormalization in magnetic field,[11] the excitonic effects in a dense electron system,[5,6,9,10] and the oscillations of the intersubband relaxation of photoexcited nonequilibrium electrons.[7,8]

Here we study the PL at a quantizing magnetic field of the electron system in a WSQW with front and back gates for changing its potential profile in the z direction. Such a design of the sample allows us to precisely position the bottom of the second electron subband *right above* the Fermi level and to gradually drive the electron system from the single-to double-layer regime. In this case we observe at low temperatures $\lesssim 600$ mK magneto-oscillations of the second-electron-subband PL intensity with maxima near odd filling factors, which vanish at higher temperatures of the order of the electron Zeeman energy.

The studied WSQW structure consists of an 80 nm wide GaAs quantum well confined by Al$_{0.35}$Ga$_{0.65}$As barriers with remote doping (for details see Ref. 1). A standard Hall bar with a semitransparent NiCr Schottky front gate was fabricated. The sample was mounted in the mixing chamber of a ^{3}He/^{4}He dilution refrigerator with a base temperature $T_{bath} = 40$ mK. The sample was excited by a cw semiconductor laser with photon energy below the barrier gap ($\lambda = 770$ nm), and excitation density $W_{ex} \approx 10^{-5}$ W/cm^2. Excitation and collection of the PL signal were done by using 0.6 mm quartz fiber. Care was executed to ensure that the laser excitation spot illuminated the entire active region of the Hall bar. The PL signal from the sample was dispersed by a double grating monochromator and recorded by a charge coupled device (CCD) camera. The electron concentration and the potential profile of the WSQW were varied by front (V_{fg}) and back (V_{bg}) gate biases. The electron concentration in the WSQW was determined from transport measurements carried on simultaneously with PL.

The variation of zero magnetic-field PL spectra of the WSQW with applied gate voltages is depicted in Fig. 1. The effect of V_{bg} at a fixed $V_{fg} = +0.35$ V is shown in Fig. 1(a). Increasing V_{bg} results in the increase of the electron concentration in the WSQW, which is 1.2×10^{11} cm^{-2} at $V_{bg} = +0.7$ V and 5.5×10^{11} cm^{-2} at $V_{bg} = +4$ V, if $V_{fg} = +0.35$ V. Three lines marked A, S_1, and S_2 are seen in Fig. 1(a). The S_1 and S_2 lines correspond to the recombination of electrons from the first and the second subbands, respectively, with photoexcited holes in the WSQW. The behavior of the energies and intensities of S lines with changing gate bias reflects the change of the WSQW potential profile. In particular, the S line energies shift down with an increase of V_{bg}, however, with different rates. As electrons from the second subband have broader z components of the wave function, the S_2 line energy is less affected by the quantum-well potential variations, see Fig. 1 (a similar PL
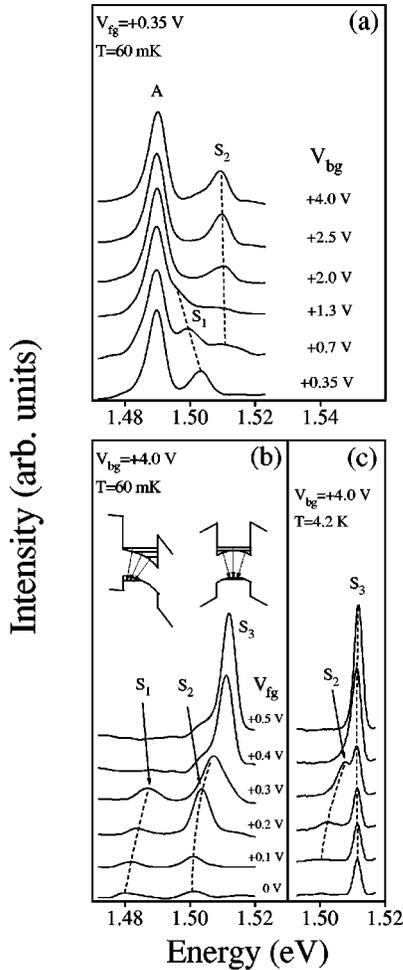
FIG. 1. Zero magnetic-field PL spectra of the WSQW at fixed V_{fg} (a) and V_{bg} (b,c). In cases (b,c) where the reference spectrum of the bulk line A measured at $V_{bg} = +4.0$ V, $V_{fg} = -0.7$ V was subtracted from the raw spectra. The dashed lines are guides to the eye. Inset: a schematic view of the WSQW potential profile for the asymmetric (left) and symmetric (right) regimes. The arrows indicate optical transitions for different electron subbands.

behavior was observed in single quantum wells with variable electron concentration[5,9]). Unlike the S lines, neither the intensity nor the energy of the A line are affected by applied bias. The A line energy (1.49 eV) falls within the region of the emission energies of donor-acceptor pairs in the bulk of GaAs, see, e.g., Ref. 4. Therefore, we attribute line A to the emission of GaAs substrate.

The effect of V_{fg} on PL spectra of the WSQW at a fixed $V_{bg} = +4$ V is shown in Figs. 1(b) and 1(c). As the S_1 line overlaps with the bulk line A and is not resolved in the spectra for $V_{bg} \gtrsim +1.3$ V [see Fig. 1(a)], the PL spectra presented in Figs. 1(b) and 1(c) have been obtained by subtracting the reference spectrum of the A line measured at $V_{bg} = +4.0$ V and $V_{fg} = -0.7$ V (at $V_{fg} = -0.7$ V the S line contribution to the PL intensity of the A line is negligible). In the studied region of gate voltages the influence of V_{fg} on the total electron concentration in the WSQW is relatively weak: if $V_{bg} = +4$ V, the total electron concentration varies from 5.2×10^{11} cm^{-2} at $V_{fg} = 0$ V to 5.6×10^{11} cm^{-2} at $V_{fg} = +0.5$ V. With the increase of V_{fg} the WSQW potential profile changes toward the symmetric one, which results in
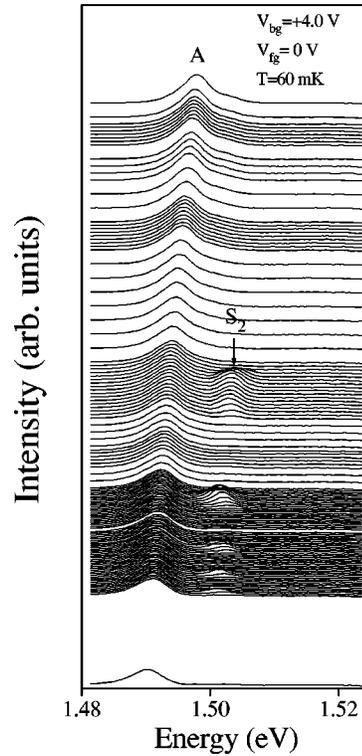

FIG. 2. PL spectra of the WSQW for magnetic fields $B = 0$ -14 T. The spectra are spaced proportionally to steps in B.

increasing the S line energies [Figs. 1(b) and 1(c)]. At $V_{fg} \gtrsim +0.4$ V line S_2 overlaps with a new line S_3, positioned at 1.511 eV. The S_3 line corresponds to the recombination of electrons from the third subband and is separately resolved only at high temperatures $\gtrsim 1.5$ K, see Fig. 1(c). The relative occupation of electron subbands can be determined from the intersubband separation (known from the S line energies) and the total electron concentration. It was found that, e.g., for $V_{bg} = +4$ V electrons start to occupy the second subband in equilibrium at $V_{fg} \gtrsim +0.3$ V.

The PL spectra of the WSQW at $V_{bg} = +4$ V, $V_{fg} = 0$ V, $T_{bath} = 60$ mK and $B = 0-14$ T are presented in Fig. 2. The intensity of the S_2 line oscillates strongly with B; the intensity oscillations are accompanied by the S_2 transition energy oscillations. In contrast, the energy and intensity of the bulk line A increase monotonically with B, as expected for the donor-acceptor emission in GaAs.[4] The corresponding intensities alongside with ρ_{xx} vs B are shown in the left part of Figs. 3(a) and 3(c). Also shown in Fig. 3(b) is the Landau-level (LL) fan diagram calculated for the effective electron mass $0.068m_0$; the electron Zeeman splitting is included for visualization purposes and does not indicate the actual value of Zeeman splitting $2sg_e\mu B$ ($s = 1/2$ is an electron spin, μ is the Bohr magneton, and g_e is the effective electron g factor), which is too small on the present energy scale. For the bare GaAs electron g factor $g_e = -0.44$, the Zeeman splitting is 0.296 K/T. The g_e enhancement near odd ν due to intra-LL (Ref. 12) and inter-LL (Ref. 13) exchange interaction is not shown in the figure. The S_2 line intensity I_{S2} enhances strongly at ν_{int} corresponding to the intersections of the zero LL of the second subband and LL's of the first subband and decreases abruptly at odd ν (Fig. 3).

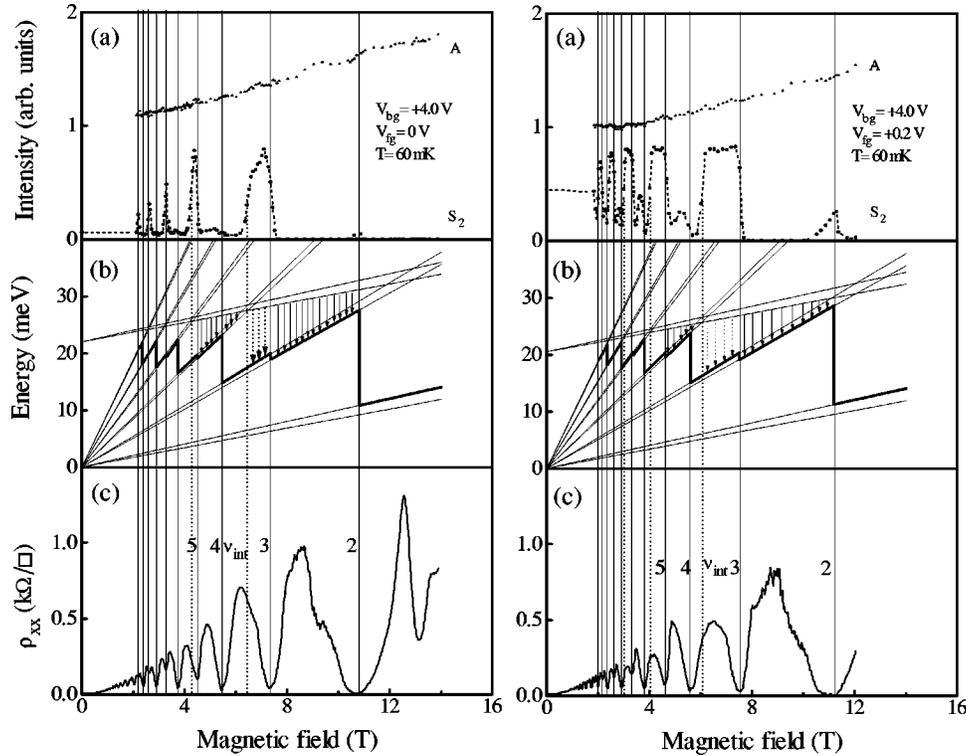The intersubband spacing can be appreciably varied by

FIG. 3. Magnetic-field dependences of the A and S_2 line intensities (a). The vertical solid lines mark integer filling factors as determined from ρ_{xx} (c). The Landau-level fan diagram is calculated for an effective electron mass $0.068m_0$ (b); the electron Zeeman splitting is included for visualization purposes and does not indicate the actual value of Zeeman splitting, see the text. The magnetic-field regions where the electron intersubband relaxation with spin conservation is allowed (forbidden) are indicated by solid (dotted) arrows. The bold line shows schematically the electron Fermi-level oscillations with B. Also shown is the definition of ν_{int}.

V_{fg} at nearly constant electron density. With reducing intersubband spacing, ν_{int} shift to lower fields, which leads to broadening the I_{S2} maxima [the right part of Fig. 3(a)]. Also, new maxima in I_{S2} emerge near even ν as seen from the figure. These additional maxima are linked to the slowing of the intersubband electron relaxation accompanied by acoustic-phonon emission because of the ''shrinkage'' of the gap between the zero LL of the second subband and the Fermi level.[7,8,14]

Since in the studied range of gate voltages the WSQW is in the single-layer regime with only one electron subband occupied in equilibrium, the observed low-temperature oscillations of I_{S2} are due to the relaxation kinetics of nonequilibrium photoexcited electrons from the second subband, i.e., to the interplay between radiation and relaxation channels. For $2 \leqslant \nu \leqslant 3$ and $\nu_{int} \leqslant \nu \leqslant 5$ electrons from the second subband can relax on empty states in the first subband with spin conservation. If $3 \leqslant \nu \leqslant \nu_{int}$, only spin flip intersubband relaxation from the lower spin state of the second subband is allowed as practically all spin states with the same spin in the first subband are occupied at $T \ll 2s g_e \mu B$. The relaxation time with spin conservation is far smaller than the one with spin flip.[8] Therefore, at $3 \leqslant \nu \leqslant \nu_{int}$ the nonequilibrium electron occupation of the second subband increases, giving rise to a maximum in I_{S2}.

When the temperature is increased, electrons in both subbands redistribute between their spin states. The appearance of both electrons in the upper spin state in the second subband and holes in the lower spin state of the first subband allows the fast intersubband relaxation with spin conserva-

tion followed by the reduction of nonequilibrium occupation of the second subband. Because of the spatial separation between the subbands' charge density maxima, the exchange enhancement of the electron g factor near odd ν due to in-
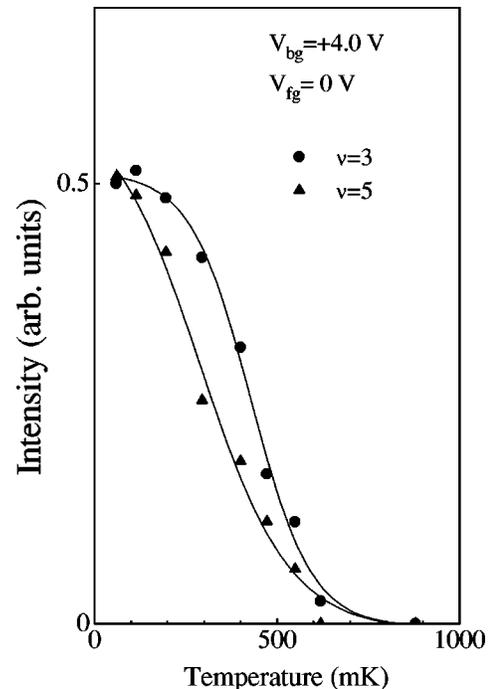

FIG. 4. Temperature dependence of the S_2 line intensity at $\nu = 3$ and 5. The solid lines are guides to the eye.

tersubband interaction is expected to be smaller than that caused by intrasubband interaction. Hence, it is the increase of occupation of the upper spin state in the second electron subband that dominates the intersubband relaxation at higher temperatures. The exchange enhancement of the spin splitting for the second subband is likely to be small because the I_{S2} oscillations are observed at temperatures $T \lesssim 600$ mK (Fig. 4), which is of the same order of magnitude as the electron Zeeman splitting. Obviously, the rigorous determination of the spin-flip activation energy from the measured temperature dependences of I_{S2} is impossible without knowing the recombination and relaxation times which are necessary parameters for the relaxation kinetic equation.

In conclusion, magneto-oscillations of the 2D electron gas PL intensity have been observed in a WSQW near the single-to double-layer transition. The simultaneous PL and transport measurements at different intersubband separations have shown that the PL intensity of the recombination of nonequilibrium electrons from the second subband enhances strongly if only a spin flip intersubband relaxation channel is open. The PL oscillations are quenched at temperatures order of the electron Zeeman energy. The found PL behavior is discussed in terms of oscillations of the second-electron-subband nonequilibrium population caused by different characteristic times for the spin-flip and spin conserving relaxation processes.

[1] Y. W. Suen, L. W. Engel, M. B. Santos, M. Shayegan, and D. C. Tsui, Phys. Rev. Lett. **68**, 1379 (1992); Y. W. Suen, H. C. Manoharan, X. Ying, M. B. Santos, and M. Shayegan, *ibid.* **72**, 3405 (1994); T. S. Lay, Y. W. Suen, H. C. Manoharan, X. Ying, M. B. Santos, and M. Shayegan, Phys. Rev. B **50**, 17 725 (1994).

[2] J. P. Eisenstein, G. S. Boebinger, L. N. Pfeiffer, K. W. West, and Song He, Phys. Rev. Lett. **68**, 1383 (1992); S. Q. Murphy, J. P. Eisenstein, G. S. Boebinger, L. N. Pfeiffer, and K. W. West, *ibid.* **72**, 728 (1994).

[3] X. Ying, S. R. Parihar, H. C. Manoharan, and M. Shayegan, Phys. Rev. B **52**, R11 611 (1995).

[4] I. V. Kukushkin and V. B. Timofeev, Adv. Phys. **45**, 147 (1996).

[5] W. Chen, M. Fritze, A. V. Nurmikko, D. Ackley, C. Colvard, and H. Lee, Phys. Rev. Lett. **64**, 2434 (1990); W. Chen, M. Fritze, W. Walecki, A. V. Nurmikko, D. Ackley, J. M. Hong, and L. L. Chang, Phys. Rev. B **45**, 8464 (1992).

[6] A. J. Turberfield, S. R. Haynes, P. A. Wright, R. A. Ford, R. G. Clark, J. F. Ryan, J. J. Harris, and C. T. Foxon, Phys. Rev. Lett. **65**, 637 (1991).

[7] V. E. Kirpichev, I. V. Kukushkin, V. B. Timofeev, V. I. Fal'ko, K. von Klitzing, and K. Ploog, Pis'ma Zh. Éksp. Teor. Fiz. **54**, 630 (1991) [JETP Lett. **54**, 636 (1991)].

[8] V. E. Zhitomirskii, I. E. Itskevich, V. E. Kirpichev, K. von Klitzing, I. V. Kukushkin, and V. B. Timofeev, Pis'ma Zh. Éksp. Teor. Fiz. **56**, 215 (1992) [JETP Lett. **56**, 213 (1992)].

[9] L. V. Kulik, A. V. Petinova, V. D. Kulakovskii, T. G. Andersson, S.-M. Wang, and A. V. Lomsadze, Phys. Rev. B **51**, 17 654 (1995).

[10] O. V. Volkov, V. E. Zhitomirskii, I. V. Kukushkin, K. von Klitzing, and K. Eberl, Pis'ma Zh. Éksp. Teor. Fiz. **64**, 719 (1996) [JETP Lett. **64**, 774 (1996)].

[11] S. Katayama and T. Ando, Solid State Commun. **70**, 97 (1989).

[12] F. F. Fang and P. J. Stiles, Phys. Rev. **174**, 823 (1968).

[13] L. V. Butov, V. D. Kulakovskii, and A. Forchel, Phys. Rev. B **48**, 17 933 (1993).

[14] V. I. Fal'ko, Phys. Rev. B **47**, 13 585 (1993).